10.1109/ULTSYM.2013.0099

Breast Imaging with Ultrasound Tomography: Initial results with SoftVue

Neb Duric, Peter Littrup, Olivier Roy, Steven Schmidt, Cuiping Li, Lisa Bey-Knight, and Xiaoyang Chen

Delphinus Medical Technologies Inc, Plymouth MI, USA and Karmanos Cancer Institute, Detroit MI

***Abstract*— The purpose of this paper is to describe the technical and clinical performance of SoftVue, a breast imaging device based on the principles of ultrasound tomography. We report on initial results from data acquired from 30 participants in a recently undertaken clinical study. Initial results suggest that SoftVue can accurately image the full range of breast anatomy, including both benign lesions and cancer. Ongoing research is focused on assessing SoftVue's ability to differentiate benign masses from cancer.**

Keywords—ultrasound; tomography; breast; imaging

I. INTRODUCTION

Over the past 30 years, a number of research groups have developed breast imaging prototypes, based on the principles of ultrasound tomography (UST). Clinical examples include the work of Carson et al. at the University of Michigan [1], Andre et al. at the University of California at San Diego [2], Johnson et al. at TechniScan Medical Systems [3], Marmarelis et al. at the University of South California [4], Liu and Waag at the University of Rochester [5], and Duric and Littrup et al. at the Karmanos Cancer Institute, Wayne State University [6,7]. More recently, Ruiter et al. [8] have reported progress on a scanner utilizing a hemispherical array of transducers. The prototypes developed by these groups used similar patient-interfaces. Patients were positioned in the prone position on a flat table with the breast suspended through a hole in the table into a water bath lying just below the table surface. The water bath ensures minimal distortion of the breast while providing strong coupling of acoustic waves to the tissue.

In our laboratories, at the Karmanos Cancer Institute (KCI), our group had focused on the development of UST breast imaging with a system that incorporates a novel ring transducer. The continuing development of the prototype and the associated UST methodology have been continuously guided by feedback from clinical studies conducted at KCI. Clinical imaging with the KCI system used previously described tomographic reconstruction algorithms that yielded (i) sound speed, (ii) attenuation, and (iii) reflection images. [7,9]. The continued research with the KCI prototype has recently transitioned to a commercial effort t with the spin out of Delphinus Medical Technologies (DMT). Building on the earlier work at KCI, DMT has developed SoftVue, a commercial-grade breast imaging device. The SoftVue scanner is pictured in Fig. 1 and its characteristics are summarized in Table 1.

Fig. 1. The SoftVue breast imaging system.

Table 1. SoftVue operating parameters	
Number of transducer elements	2048
Number of receive channels	512
Number of transmit channels	512
Operating frequency	3 MHz
Data resolution	14 bits
Image resolution (B-mode)	0.7 mm
Slice thickness	2.5mm
Max. breast diameter	22 cm
Reconstruction time per slice	15 s

II. METHODS

Following laboratory testing, SoftVue was installed at KCI's, Alexander J. Walt Comprehensive Breast Center in November, 2012. After initial comparative testing with the old prototype, we began a 100 patient study at KCI to test the clinical performance of the system. Participants were consented and data acquired under a protocol approved by Wayne State University's internal review board (approval number #040912M1F). To date, 30 patients have been scanned with SoftVue. SoftVue's image reconstruction algorithm was used to generate cross-sectional reflection B-Mode images. The reflection images were corrected for refraction and attenuation effects to maximize image quality [9]. Typically 30 to 40 tomograms (image slices) were reconstructed for each

participant. An anthropomorphic breast phantom, designed and built by Dr. Ernie Madsen (University of Wisconsin) was also imaged in order to test the accuracy of the SoftVue imaging system.

III. Results and Discussion

Extensive imaging of the breast phantom yielded information on the image reconstruction accuracy that was used to optimize system parameters. An example of a phantom image, shown in Fig. 2, reveals the skin, subcutaneous fat, glandular tissue, an 8mm cancer, a 12mm cyst, a 12mm fibroadenoma and a group of 500 micron sized microcalcifications.

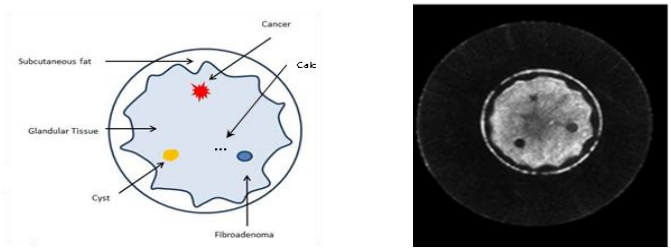

Fig. 2. Imaging an anthropomorphic breast phantom.

A visual comparison of the phantom image with the known properties of the phantom showed that the geometry and contents of the phantom were accurately reproduced with measurement uncertainties ranging from 0.2 to 0.5 mm. These uncertainties are within the 0.7 mm spatial resolution of the system.

Following the phantom imaging studies, we successfully obtained 30 in-vivo data sets from our ongoing SoftVue study participants. The corresponding image stacks were analyzed to characterize SoftVue's ability to detect and render general breast anatomy. The first element of that analysis was to investigate the imaging performance as a function of breast density. We binned participant images according to the BIRADS density categories of 1 through 4 and examined the images for systematic trends in sensitivity and accuracy of anatomical rendering. Examples are shown in Figure 3 where we have ordered representative images based on the 4 BIRADS density categories. It can be seen that, for increasing breast density, the underlying breast architecture of fibrous bands and/or Cooper's ligaments become less and less visible as the enveloping parenchymal tissue contributes to the increasing radiographic appearance. In more fatty breasts, the specular reflectors of the fibrous bands are thus readily identified while the non-specular echo signals from the extended denser tissues dominate the images of the denser breasts. This behavior with density mimics that of mammography as far as overall breast anatomy is concerned and indicates that SoftVue's is able to image anatomy even in dense breasts.

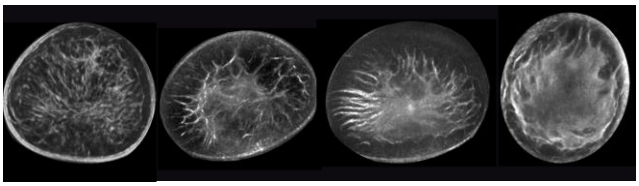

Fig. 3. Representative coronal cross-sections of SoftVue images for partcipants with increasing breast density (from left to right).

The next step in the analysis was to determine the accuracy with which breast anatomy is rendered. For our gold standard, we used MRI images. MRI is an ideal standard because it images the whole pendant breast in a geometry that is similar to that of SoftVue. Furthermore, MRI images can be reconstructed in coronal planes, thereby allowing for a direct comparison with SoftVue. Such comparisons were successfully carried out by our group with the earlier research prototypes [10]. Two examples of such a comparison are shown in Fig. 4 and 5, comparing breast anatomy for a similar region of the breast and showing good agreement.

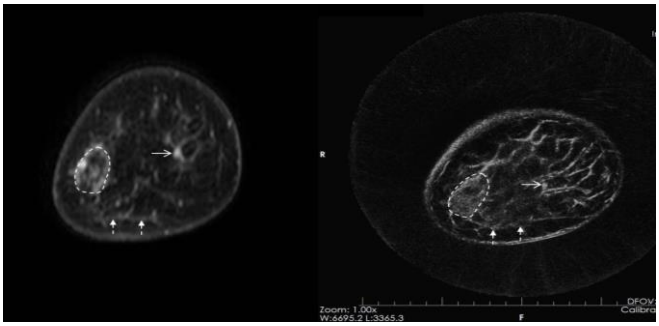

Fig. 4. Comparisons of normal architecture on enhanced T1-weighted fat-subtracted MR reconstructed in the coronal plane (left) with SoftVue image (right) at similar slice level. The mild differences in outer breast contours relate to effects of gravity for the prone breast in air on MR, while gravity has little effect upon the breast in water for SoftVue. Details are highlighted for a region of parenchyma (dashed oval) which has slightly greater vascularity on MR and echogenicity by SoftVue. Note the identical oval contours were only rotated to a similar extent as the outer breast contours to match the echogenic region on UST, as well as other matching anatomic foci (arrows).

Figure 5 compares abnormal anatomy arising from post-lumpectomy architectural distortion, again, showing good agreement.

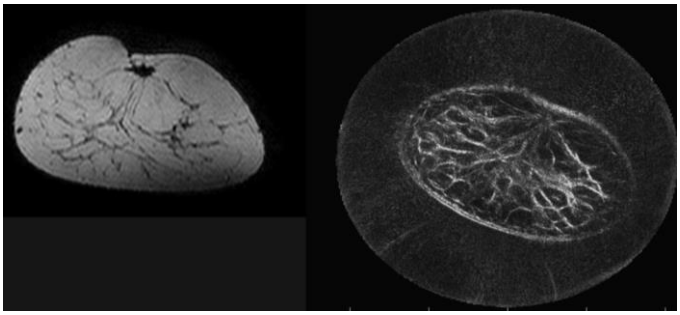

Fig. 5. 51 year old post-lumpectomy with no evidence of recurrence and only residual architectural distortion in the 1 o'clock position as seen on non-enhanced T1-weighted MR image (left). SoftVue (right) shows corresponding distortion (arrow) in the coronal plane.

The third element of the analysis focused on the imaging of masses across the breast density continuum. Our sample of study participants with findings included fibroadenomas, cysts and cancers. As in conventional ultrasound, we found that masses are not obscured by dense parenchyma, due to their differences in biomechanical, and therefore acoustic, properties relative to background tissue.

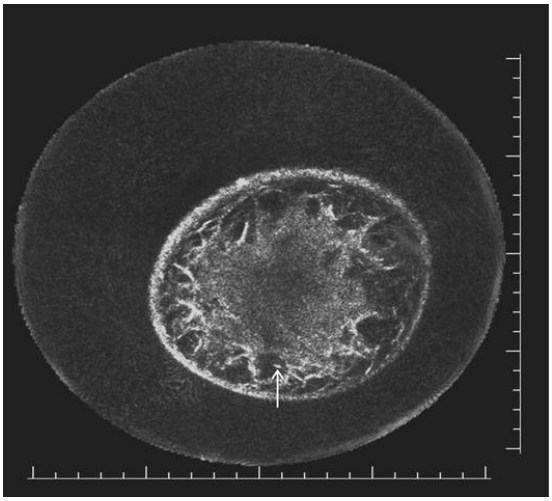

Fig. 6. 45 year old with a 1cm invasive ductal carcinoma at the 6 o'clock position also showing the clip from prior biopsy (arrow).

Figure 6 shows a 1.4 cm cancer, which is embedded in dense parenchyma. The biopsy clip inside the mass can also be seen. Figure 7 shows an example of a 2 cm cancer also embedded in dense parenchyma.

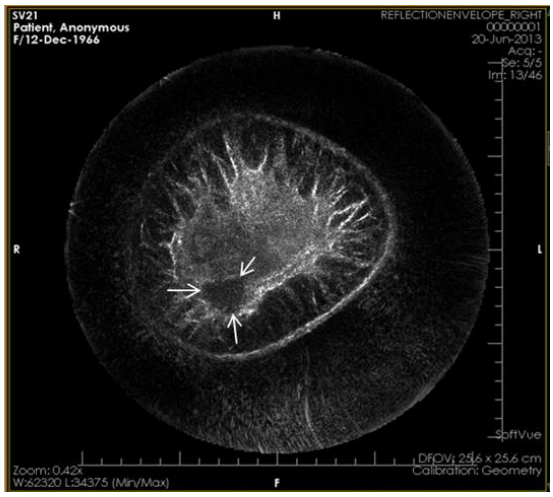

Fig. 7. Example 46 year old woman with a newly diagnosed 2.3 x 2.5 cm invasive ductal carcinoma (large arrows) at the 7 o'clock position

Examples of benign masses are shown in Fig. 8 (a cyst), Fig. 9 (coarse calcification), and Fig. 10 and 11 (fibroadenomas). In all cases, masses were characterized by their hypoechoic signature relative to background tissue, even in cases where the breast tissue is very dense.

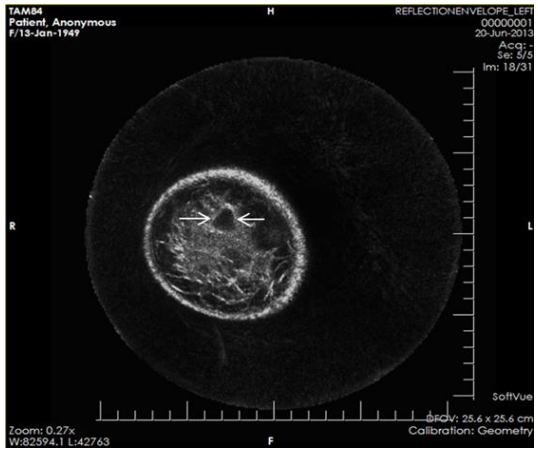

Fig. 8. 62 year old woman with a cyst (arrows) at the 12 o'clock position.

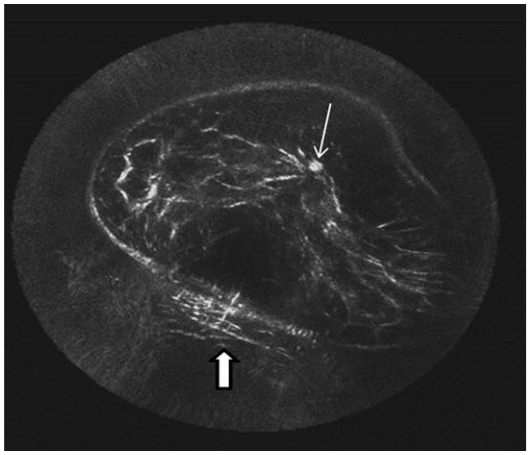

Fig. 9. 51 year old with no evidence of recurrence and only residual architectural distortion near 1 o'clock. Arrow points to the dystrophic coarse calcification in the lumpectomy site. Note also the skin roll (block arrow) caused by loose tissue near the chest wall.

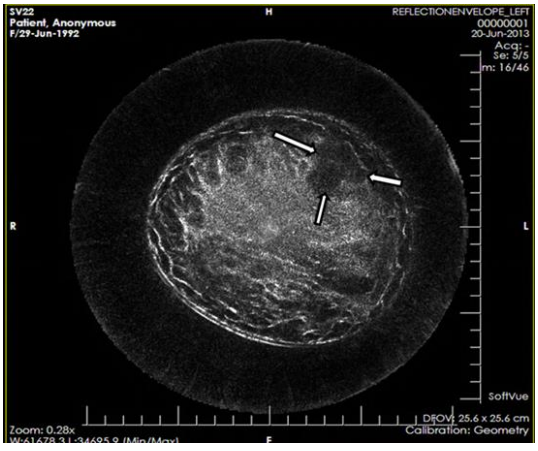

Fig. 10. 21 year-old with palpable mass in the 1:00 position of the left breast, which corresponded to a 3.4 x 2.7 cm lobulated hypoechoic region (arrows). Subsequent biopsy confirmed fibroadenoma.

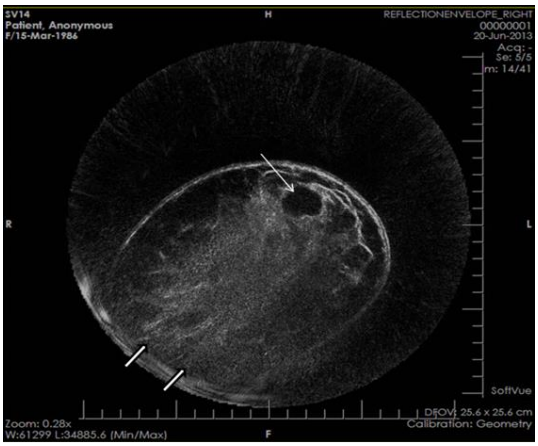

Fig. 11. 26 year-old with palpable mass near the 12:00 o'clock position of the left breast, which corresponded to a 2.0 cm mildly lobulated hypoechoic region (arrow). Subsequent biopsy confirmed fibroadenoma. Block arrows demonstrate distortion from breast touching the transducer in the 6-9:00 position.

Figure 12 illustrates results from ongoing research aimed at adding information from transmission images [11]. The Image on the left is a reflection (B-mode) image of the breast and tumor. The image on the right has (i) a grey-scale sound speed image overlay (to accentuate dense tissues) and (ii) pixel colorization to accentuate regions with high values of attenuation and sound speed.

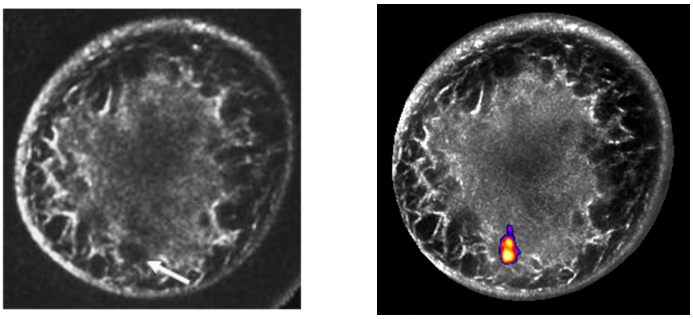

Fig. 12. 45 year old with a 1cm invasive ductal carcinoma at the 6 o'clock position (arrow). The fusion image on the right shows the dense tissues (grey), fat (black) and a stiff solid mass corresponding to the carcinoma (color).

IV. Conclusions

Initial results suggest that SoftVue can accurately image the full range of breast anatomy, along with both benign lesions and cancer. Ongoing research is focused on validating and quantifying these findings in a larger sample of study participants. Future research will aim to assess SoftVue's ability to differentiate benign masses from cancer.

V. Acknowledgments

The research presented in this paper is supported, in part, through an SBIR grant 1R44CA165320 from the National Cancer Institute.

VI. Disclosures

All imaging procedures were performed under an Institutional Review Board (IRB) approved research protocol and in compliance with the Health Insurance Portability and Accountability Act (HIPAA). All investigators have financial interests in Delphinus Medical Technologies. SoftVue is not yet cleared by the FDA and does not yet have a CE mark.

References

[1] Carson, P. L., Meyer, C. R., Scherzinger, A. L. & Oughton, T. V., 1981. Breast imaging in coronal planes with simultaneous pulse echo and transmission ultrasound.. Science, 4 Dec, 214(4525), pp. 1141-1143.

[2] Andre, M. P. et al., 1997. High-speed data acquisition in a diffraction tomography system employing large-scale toroidal arrays. International Journal of Imaging Systems and Technology , 8(1), pp. 137-147..

[3] Johnson, S. A. et al., 1999. Apparatus and Method for Imaging with Wavefields using Inverse Scattering Techniques. United States of America, Patent No. 6,005,916.

[4] Marmarelis, V. Z., Kim, T. & Shehada, R. E., 2003. High resolution ultrasonic transmission tomography. San Diego, California, SPIE, pp. 33-40.

[5] Liu, D.-L. & Waag, R., 1997. Propagation and backpropagation for ultrasonic wavefront design. IEEE Transactions on Ultrasonics, Ferroelectrics and Frequency Control, January, 44(1), pp. 1-13.

[6] Duric, N. et al., 2007. Detection of breast cancer with ultrasound tomography: first results with the Computed Ultrasound Risk Evaluation (CURE) prototype.. Medical Physics, February, 34(2), pp. 773-785.

[7] Li, C., Duric, N., Littrup, P. & Huang, L., 2009. In vivo breast sound-speed imaging with ultrasound tomograph. Ultrasound in Medicine & Biology, October, 35(10), pp. 1615-1628.

[8] Ruiter, N. V. et al., 2011. Realization of an optimized 3D USCT. Lake Buena Vista, Florida, SPIE, pp. 796805-1-8.

[9] Schmidt, S. et al., 2011. Modification of Kirchhoff Migration with Variable Sound Speed and Attenuation for Tomographic Imaging of the Breast. Lake Buena Vista, Florida, SPIE, pp. 796804-1-11..

[10] Ranger B, Littrup P, Duric N, Chandiwala-Mody P, Li C, Schmidt S and Lupinacci J. Breast ultrasound tomography versus magnetic resonance imaging for clinical display of anatomy and tumor rendering: Preliminary results. AJR Am J Roentgenol 2012; 198:233–239.

[11] Greenleaf, J., Johnson, S., Bahn, R. & Rajagopalan, B., 1977. Greenleaf JF, JohnsoQuantitative cross-sectional imaging of ultrasound parameters. s.l., IEEE Cat. # 77, pp. 989-995.